

# Operation Mechanism and Efficiency-Limiting Factors in Quantum-Dot Light-Emitting Diodes

Hiroyoshi Naito<sup>1,2</sup>

naito@pe.osakafu-u.ac.jp (H. Naito)

<sup>1</sup> Department of Physics and Electronics, Osaka Prefecture University, Sakai, 599-8531, Japan

<sup>2</sup> The Research Institute for Molecular Electronic Devices, Osaka Prefecture University, Sakai, 599-8531, Japan

Keywords: Quantum-dot; Quantum-dot light-emitting diode; Operation mechanism; Efficiency-limiting factors

## ABSTRACT

*Efficiency limiting factors and operation mechanism of quantum dots light-emitting diodes (QLEDs) are studied by means of machine learning, device simulation and experiments. The factors and the mechanism of QLEDs are shown and the importance of the characterization of the electronic transport properties of QLEDs is also shown.*

## 1 Introduction

Quantum dots (QDs) are solution-processed semiconductor nano-crystals that feature narrow band emission, size-tunable band-gaps, and high photoluminescence quantum efficiency [1]. The QDs are thereby good materials for use in 8K displays [2–11]. For the rea-sons, a number of research toward high performance light-emitting diodes based on QDs (quantum-dot light-emitting diodes: QLEDs) has been extensively performed [2–23].

Typical structure of solution-processed QLED is ITO/HIL/HTL/QD/ETL/Al and is shown in Fig. 1, where ITO is indium tin oxide transparent anode, HIL is hole injection layer, HTL is hole transport layer, ETL is electron transport layer (printable ZnO nanoparticles were used as ETL in literature), and Al is the cathode. The maximum current efficiencies of red, green and blue QLEDs using Cd based QD with the device structure in Fig. 1 were reported to be 9.24 cd A<sup>-1</sup>, 27.98 cd A<sup>-1</sup>, 1.49 cd A<sup>-1</sup>, respectively [11]. Consequently, operation mechanisms and efficiency-limiting factors of the QLEDs in Fig. 1 are an important issue [12].

In this presentation, first we examine efficiency-limiting factors of the QLEDs whose device structure is shown in Fig. 1 in terms of machine learning approach based on the data collected from literature. Second, we carry out device simulation to understand operation mechanism of the QLEDs by taking account of the efficiency-limiting factors revealed by the machine learning. Third, we examine the consistency between the operation mechanism and the experimentally-observed behavior of the QLEDs. Finally, we show other efficiency-limiting factors of the QLEDs, which are not taken into account in the machine learning.

## 2 Efficiency-limiting factors of QLEDs: machine learning study

The random forest regression using the data of 100

QLEDs collected from 55 papers (see Supplemental information in Ref. [12]) shows that the energy level of the valence band edge of the QD layer has the highest importance, and the HOMO energy levels of the HIL and the HTL have higher importance, shown in Fig. 2. The results indicate that hole injection from the HTL to the QD layer is the most important efficiency-limiting factor of QLEDs. The results also indicate that Förster energy migration of excitons formed in HTL to QDs does not play an important role.

## 3 Experiment

QLEDs with the structure shown in Fig. 1 were fabricated using printing processes. Poly(ethylenedioxythiophene):polystyrene sulpho-nate (PEDOT:PSS) was used for HIL, and poly(9,9-dioctyluorene-co-N-(4-(3-methylpropyl))diphenylamine) (TFB) or poly(9-vinylcarbazole) (PVK) used for HTL [12].

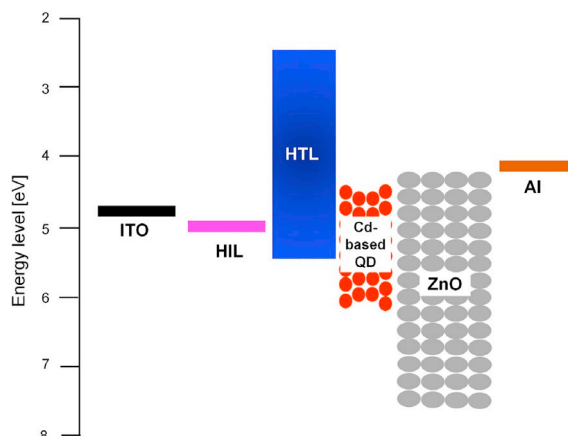


**Fig. 1. Typical structure of solution-processed QLED with Cd-based QDs [14, 16,17].**

## 4 Results and discussion

### 4.1 Device performance of QLEDs

The  $J$ - $V$  and luminescence-voltage ( $L$ - $V$ ) characteristics of the QLED with TFB, where HOMO level of TFB is 5.3 eV, are shown in Fig. 2. The maximum luminances for the QLED with TFB reached as high as ~10500 cd m<sup>-2</sup>, and the maximum current efficiency was 1.57 cd A<sup>-1</sup>.

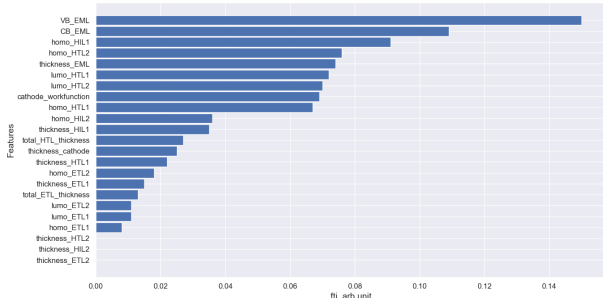


**Fig. 2. Feature importance based on the random forest regression [12]**

Fig. 3 shows PL spectrum of the QDs thin film and the EL spectrum of QLEDs. The emission peak and the full-width at half-maximum (FWHM) of the PL and the EL spectra are located at 619 nm and about 30 nm, respectively. We also fabricated QLEDs with the structure of ITO/PEDOT:PSS/PVK/PEI/QDs/ZnO/Al to reduce the hole injection barrier, where PEI is polyethylenimine, and HOMO level of PVK is 5.8 eV, which is 0.5 eV smaller than that of TFB. As we expect from the machine learning study mentioned above, the maximum luminance and the maximum current efficiency of the QLED with PVK were improved to be  $\sim 28000$  cd m<sup>-2</sup>, and 8.26 cd A<sup>-1</sup>, respectively.

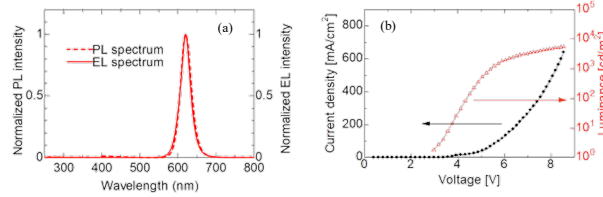


**Fig. 3. (a) J-L-V characteristics of the QLED with TFB as HTL. (b) PL spectrum of QD thin film and EL spectrum of QLED.**

**4.2 Operation mechanism in QLED**

We study operation mechanism of QLEDs using device simulation software Atlas (Silvaco, Inc.). In the device simulation, the energy levels such as highest occupied molecular orbitals (HOMOs) and lowest un-occupied molecular orbitals (LUMOs) of TFB, and the conduction band and the valence band edges of QDs and ZnO, shown in Fig. 1, were used, and the electron and hole drift mobilities of TFB (hole:  $1.0 \times 10^{-3}$ , electron:  $1.0 \times 10^{-5}$  cm<sup>2</sup>V<sup>-1</sup>s<sup>-1</sup>) and ZnO (electron:  $1.0 \times 10^{-3}$  cm<sup>2</sup>V<sup>-1</sup>s<sup>-1</sup>) reported in the literature [13,28–30] were used. The dielectric constants of TFB and ZnO were 3 and 10.6, respectively [25, 26]. The other physical quantities used in the device simulation were electron and hole mobilities of QD of 100 and 10 cm<sup>2</sup> V<sup>-1</sup> s<sup>-1</sup>, respectively, and the thickness of TFB, QD and ZnO layers of 20 nm, 10 nm and 30 nm, respectively. Since the values of the electron and the hole mobilities of QDs are not found in literature, we used those reported in crystalline CdSe [27]. We changed the mobility values

from  $1.0 \times 10^3$  to  $100$  cm<sup>2</sup> V<sup>-1</sup> s<sup>-1</sup> for

QDs and found that the band diagrams (shown in Fig. 4) of QLEDs derived from the device simulation are qualitatively the same. Fig. 4 shows the band diagrams of QLED derived from the device simulation at different bias voltages. It is found that the energy band level of HTL layer is greatly shifted downward with respect to the energy level of QD layer because of the strong electric field formed between holes in HTL and electrons in QD layer at the interface between HTL and QD layer. The energy barrier between HTL and QD layer for holes is reduced with increasing applied voltages and hence holes are injected to the QD layer above 1 V, as shown in Figs. 4(a)–4(d). Such high electric field in the QD layer can be detected by examining EL spectra of PLEDs fabricated in this study at different applied voltages, which are shown in Fig. 5. Fig. 5(b) shows the enlarged EL spectra around the EL peaks and EL peaks are red-shifted with increasing applied voltage. Electric-field induced red shift has been known as quantum-confined Stark effect [31–33], which has been observed in CdSe nano-crystallite QDs [31]. The red shift becomes obvious above  $5 \times 10^4$  Vcm<sup>-1</sup> [32] and is an indication of strong electric field in the QD layer.

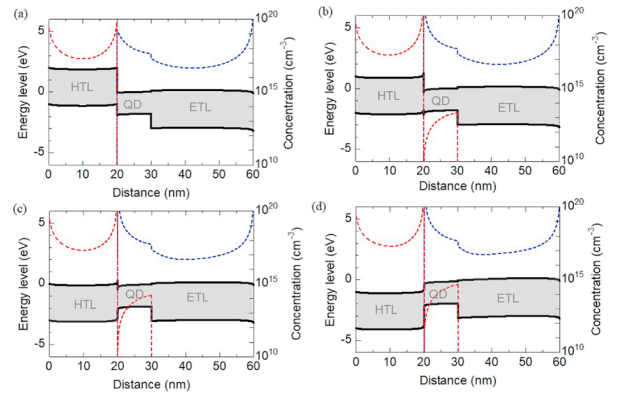


**Fig. 4. Energy diagram (gray shading indicates the bandgap) and distributions of electron (blue dotted line) and hole (red dotted line) drawn from the device simulation at the external applied voltage of (a) 1.0 V, (b) 2.0 V, (c) 3.0 V and (d) 4.0V. The origin of energy level is the conduction band edge of QD layer.**

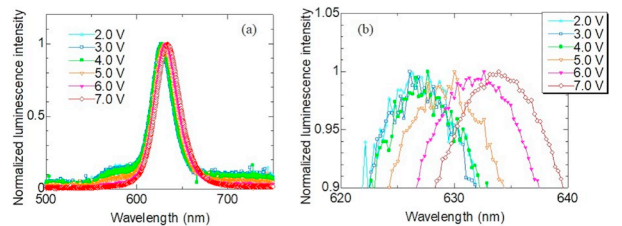


**Fig. 5. EL spectra of QLED under forward bias between 2 V–7 V.**

### 4.3 Other efficiency-limiting factors in QLEDs

We found other efficiency-limiting factors in QLEDs through the course of the data collection for the machine learning study. Fig. 6 shows the relation between the current efficiency and hole injection barrier of QLEDs with different HTLs in literature [34]. Although we observed the improvement of the current efficiency by reducing the hole injection barrier in the QLEDs with TFB or PVK as HTL, we found from Fig. 6 that the reduction in the hole injection barrier does not necessarily contribute to the improvement of the current efficiency. We see that the current efficiency was improved in case where the electron mobility of the HTLs is immeasurably small. We also see that the current efficiency is not improved at all in case of HTLs whose electron mobility is relatively high. The importance of the electron mobility of HTL is obvious from the device simulation in Fig. 4; injected electrons in QDs from ZnO can be transported to HTL without recombination above 3 V. When the electron mobility of HTL is high, electrons in QDs are efficiently extracted and hence the current efficiency is lowered. Thus, the electron mobility of HTL is an efficiency-limiting factor.

The results of the device simulation in Fig. 4 also tells us that carrier balance in the QD layer is an efficiency-limiting factor; as electron and hole densities in the QD layer become comparable, the current efficiency of QLEDs becomes maximum. To take account of the efficiency-limiting factors mentioned above in machine learning studies for the design of highly efficient QLEDs, the characterization of the transport properties of HTL, QD layer and ETL is essential, and we stress that impedance spectroscopy is a powerful tool for the characterization of transport properties in such thin semiconducting layers (10–30 nm) [37–39]. Here, instead of tuning the transport properties of HTL, QD layer and ETL in QLEDs, thin PVK layer was inserted in between the QD layer and ZnO to demonstrate the importance of the carrier balance in the QD layer. We fabricated QLEDs with the structure of ITO/PEDOT:PSS (~40 nm)/PVK (~20 nm)/PEI/QDs (~10 nm)/PVK/ZnO (~30 nm)/Al (50 nm). The current efficiency of the QLEDs of  $16.6 \text{ cdA}^{-1}$  and the maximum luminance of  $5000 \text{ cdm}^{-2}$  were obtained at the optimized PVK thickness of ~18 nm. Since the inserted PVK thin layer reduces the electron density in the QD layer, the improvement of the current efficiency is due to that of the carrier balance in the QD layers. Such simple strategy based on the device simulation results in Fig. 4 significantly improves the current efficiency of the QLEDs with thin PVK inserted layer and the current efficiency is higher than that red-emissive CdSe QD based QLEDs with the device structure in Fig. 1 re-reported in literature [11,40,41]

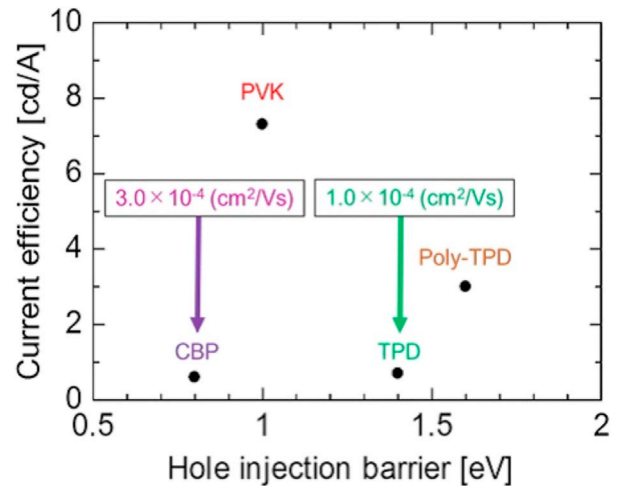


**Fig. 6. Relation between the current efficiency of QLEDs and hole injection barrier in the QLEDs with different HTLs. Poly-TPD is poly(4-butylphenyldipheyl-amine), CBP is 4,4'-bis(carbazole-9-yl)-biphenyl, and TPD is N,N'-diphenyl-N,N'-bis-(3-methylphenyl)-1,1'-diphenyl-4,4'-diamine [34]. The values shown in the figure are electron mobilities [35,36]. The electron mobilities of PVK and poly-TPD have not been reported mainly because the electron mobilities of the HTLs are immeasurably small.**

### 5 Conclusions

We studied efficiency limiting-factors and operation mechanism of CdSe based prototypical QLEDs whose device structure was ITO/HIL/HTL/QDs/ETL/Al. Information concerning the electronic transport properties of HTL, QD, and ETL is essential to the precise prediction of QLED performance using device simulation. Further extensive studies of the electronic transport measurements of these materials should be carried out using impedance spectroscopy. To do this, the development of impedance spectrometer with fast data acquisition time is a central issue for the electronic characterization of a vast class of the materials.

### Acknowledgments

This work was supported by JSPS KAKENHI Grant Numbers JP19H02599, JP20H02716, JP20K21007, and JP21H04564.

### References

- [1] Y. Shirasaki, G. J. Supran, M. G. BAwendi, V. Bulovic, *Nat. Photon.* 7 (2013) 13.
- [2] J. T. Seo, J. Han, T. Lim, K. H. Lee, J. Hwang, H. Yang, S. Ju, *ACS Nano* 8 (2014) 12476.
- [3] A. Rizzo, M. Mazzeo, M. Palumbo, G. Lerario, S. D. Amone, R. Cingolani, G. Gigli, *Adv. Mater.* 20 (2008) 1886.
- [4] T. H. Kim, K. S. Cho, E. K. Lee, S. J. Lee, J. Chae, J. W. Kim, D. H. Kim, J. Y. Kwon, G. Amarantunga,

- S. Y. Lee, B. L. Choi, Y. Kuk, J. M. Kim, K. Kim, *Nat. Photon.* 5 (2011) 176.
- [5] M. K. Choi, J. Yang, K. Kang, D. C. Kim, C. Choi, C. Park, S. J. Kim, S. I. Chae, T. H. Kim, J. H. Kim, T. Hyeon, D. H. Kim, *Nat. Commun.* 6 (2015) 7149.
- [6] L. Kim, P. O. Anikeeva, S. A. Coe-Sullivan, J. S. Steckel, M. G. Bawendi, V. Bulovic, *Nano Lett.* 8 (2008) 4513.
- [7] V. Wood, M. J. Panzer, J. Chen, M. S. Bradley, J. E. Halpert, M. G. Bawendi, V. Bulovi, *Adv. Mater.* 21 (2009) 2151.
- [8] V. L. Colvin, M. C. Schlamp, A. P. Alivisatos, *Nature* 370 (1994) 354.
- [9] X. Dai, Z. Zhang, Y. Jin, Y. Niu, H. Cao, X. Liang, L. Chen, J. Wang, *Nature* 515 (2014) 96.
- [10] H. Zhang, H. R. Li, X. W. Sun, S. M. Chen, *ACS Appl. Mater. Interfaces* 8 (2016) 5493.
- [11] H. Peng, Y. Jiang, S. Chen, *Nanoscale* 8 (2016), 17765.
- [12] S. Sano, T. Nagase, T. Kobayashi, H. Naito, *Org. Electron.* 86 (2020) 105865.
- [13] J. Yang, J. Lee, J. Lee, T. Park, S. J. Ahn, W. Yi, *Diam. Relat. Mater.* 73 (2017) 154.
- [14] F. Zhang, S. Wang, L. Wang, Q. Lin, H. Shen, W. Cao, C. Yang, H. Wang, L. Yu, Z. Du, J. Xue, L. S. Li, *Nanoscale* 8 (2016) 12182.
- [15] J. M. Carugem, J. E. Halpert, V. Wood, V. Bulovic, M. G. Bawendi, *Nat. Photon.* 2 (2008) 247.
- [16] J. Wu, Y. Deng, X. Zhang, J. Xia, W. Lei, *Org. Electron.* 58 (2018) 191.
- [17] K. Sun, F. Li, Q. Zeng, H. Hu, T. Guo, *Org. Electron.* 63 (2018) 65.
- [18] P. O. Anikeeva, C. F. Madigan, J. E. Halpert, M. G. Bawendi, V. Bulovic, *Phys. Rev. B* 78 (2008), 085434.
- [19] Y. Q. Zhang, X. A. Cao, *Appl. Phys. Lett.* 97 (2010) 253115.
- [20] P. T. K. Chin, R. A. M. Hikmet, R. A. J. Janssen, *J. Appl. Phys.* 104 (2008) 013108.
- [21] Y. Liu, C. Jiang, C. Song, J. Wang, L. Mu, Z. He, Z. Zhong, Y. Cun, C. Mai, J. Wang, J. Peng, Y. Cao, *ACS Nano* 12 (2018) 1564.
- [22] D. Kim, Y. Fu, S. Kim, W. Lee, K. H. Lee, H. K. Chung, H. J. Lee, H. Yang, H. Chae, *ACS Nano* 11 (2017) 1982.
- [23] Y. Fu, W. Jiang, D. Kim, W. Lee, H. Chae, *ACS Appl. Mater. Interfaces* 10 (2018) 17295.
- [24] S. Sato, M. Takata, M. Takada, H. Naito, *J. Nanosci. Nanotechnol.* 16 (2016) 3368.
- [25] S. Sato, M. Takada, D. Kawate, M. Takata, T. Kobayashi, H. Naito, *Jpn. J. Appl. Phys.* 58 (2019) SFFA02.
- [26] I. B. Kobiakov, *Solid State Commun.* 35 (1980) 305.
- [27] A. B. Fowler, *J. Phys. Chem. Solid.* 22 (1961) 181.
- [28] S. R. Tseng, Y. S. Chen, H. F. Meng, H. C. Lai, C. H. Yeh, S. F. Horng, H. H. Liao, C. S. Hsu, *Synth. Met.* 159 (2009) 137.
- [29] J. Kwak, W. K. Bae, D. Lee, I. Park, J. Lim, M. Park, H. Cho, H. Woo, D. Y. Yoon, K. Char, S. Lee, C. Lee, *Nano Lett.* 12 (2012) 2362.
- [30] W. D. Gill, *J. Appl. Phys.* 43 (1972) 12.
- [31] S. A. Empedocles, M. G. Bawendi, *Science* 278 (1997) 2114.
- [32] J. Zhao, J. A. Bardecker, A. M. Munro, M. S. Liu, Y. Niu, I.-K. Ding, J. Luo, B. Chen, A. K.-Y. Jen, D.S. Ginger, *Nano Lett.* 6 (2006) 463.
- [33] M. Fox, *Optical Properties of Solids*, second ed., Oxford University Press, New York, 2010.
- [34] M. D. Ho, D. Kim, N. Kim, S. M. Cho, H. Chae, *ACS Appl. Mater. Interfaces* 5 (2013) 12369.
- [35] H. Beak, C. Lee, B. D. Chin, *Synth. Met.* 162 (2012) 2355.
- [36] R. A. Klenkler, G. Voloshin, *J. Phys. Chem. C* 115 (2011) 16777.
- [37] T. Okachi, T. Nagase, T. Kobayashi, H. Naito, *Jpn. J. Appl. Phys.* 47 (2008) 8965.
- [38] T. Okachi, T. Nagase, T. Kobayashi, H. Naito, *Appl. Phys. Lett.* 94 (2009) 043301.
- [39] K. Takagi, T. Nagase, T. Kobayashi, H. Naito, *Appl. Phys. Lett.* 108 (2015) 053305.
- [40] J. Chen, D. Song, Z. Xu, S. Zhao, B. Qiao, W. Zheng, P. Wang, X. Zheng, W. Wu, *Org. Electron.* 75 (2019) 105412.
- [41] P. Gao, X. Lan, J. Sun, J. Huang, Y. Zhang, *J. Mater. Sci. Mater. Electron.* 31 (2020) 2551.